Compounds of paired electrons and lattice solitons moving with supersonic velocity

D. Hennig,[1,2] M. G. Velarde,[1] W. Ebeling,[1,2] and A. Chetverikov[1]
[1]*Instituto Pluridisciplinar, Universidad Complutense, Paseo Juan XXIII, 1, Madrid-28040, Spain*
[2]*Institut für Physik, Humboldt-Universität Berlin, Newtonstrasse 15, Berlin 12489, Germany*
(Received 14 August 2008; published 16 December 2008)

We study the time evolution of two correlated electrons of opposite spin in an anharmonic lattice chain. The electrons are described quantum mechanically by the Hubbard model while the lattice is treated classically. The lattice units are coupled via Morse-Toda potentials. Interaction between the lattice and the electrons arises due to the dependence of the electron transfer-matrix element on the distance between neighboring lattice units. Localized configurations comprising a paired electron and a pair of lattice deformation solitons are constructed such that an associated energy functional is minimized. We investigate long-lived, stable pairing features. It is demonstrated that traveling pairs of lattice solitons serve as carriers for the paired electrons realizing coherent transport of the two correlated electrons. We also observe dynamical narrowing of the states, that is, starting from an initial double-peak profile of the electron probability distribution, a single-peak profile is adopted going along with enhancement of localization of the paired electrons. Interestingly, a parameter regime is identified for which supersonic transport of paired electrons is achieved.

DOI: 10.1103/PhysRevE.78.066606 PACS number(s): 05.45.Yv, 87.10.Hk, 63.20.Ry

I. INTRODUCTION

Since the pioneering work of Landau and Pekar, it has been established that when an electron in a lattice interacts locally with the phonons it can become self-trapped by the lattice distortion it creates [1,2]. The generated quasiparticle consisting of the localized electron and its associated local lattice deformation is called a polaron (an electron surrounded by a phonon cloud). Fröhlich (large polarons) and Holstein (small polarons) elaborated significantly on the consequences of the polaron concept [3,4]. Further significant work was done by several other authors [5], in particular by Feynman, who developed the path-integral methodology [6]. Later this idea of a localized quasiparticle was used by Davydov to propose a model for coherent energy and/or charge transport in macromolecules [7–12].

Recently, Cruzeiro-Hansson *et al.* [13] have considered a generalized Davydov Hamiltonian augmented with both attractive and repulsive Coulomb interaction between generic "quasiparticles" (hole or electron) modeling spin-spin interaction or Coulomb repulsion and using Hubbard's local Hamiltonian [14]. Two kinds of nonlinearity were incorporated in the dynamics. One nonlinearity comes from the polaronic electron-lattice interaction (called extrinsic nonlinearity). The other kind of nonlinearity, called intrinsic, was twofold because it considered the $1/r^{12}$ Lennard-Jones (LJ) repulsive interaction between lattice units and also took the units as on-site nonlinear oscillators with quartic potential. The latter offers naturally the possibility of exciting "breathers" along the lattice. Figure 1 shows the LJ potential compared to the Morse and Toda repulsive exponential interactions. The Lennard-Jones potential is closely related to the Toda and the Morse potential with respect to linear and (small) nonlinear excitations. The common feature is the fact that these two-parameter potentials have an asymmetric minimum with a negative third derivative. By scaling the two parameters, the frequency of linear oscillations and the stiffness may be mapped to each other. After adapting the second and third derivatives, one may expect that the linear and the (small) nonlinear excitations are closely related. As shown by [15–17], interactions with these properties have in common the existence of supersonic solitonic excitations with specific properties. We have demonstrated the existence of such excitations and their influence on the electron dynamics in previous work. Cruzeiro-Hansson *et al.* analyzed the perturbation of the single polaron state induced by the presence of a second quasiparticle with opposite spin. Thus the question studied was the influence of the strength and sign of the Hubbard (local) interaction on the evolution of paired quasiparticle states. They also analyzed in detail the role of the $1/r^{12}$ LJ anharmonicity versus the harmonic approximation upon the evolution of such paired states. One of their findings is that within a certain range of parameters, the states in which the two quasiparticles are paired and coupled to a discrete breather are energetically more favorable than those of uncorrelated quasiparticles.

Another study of the role of the Hubbard repulsion in a Fröhlich/Holstein-Davydov kind of problem worth recalling

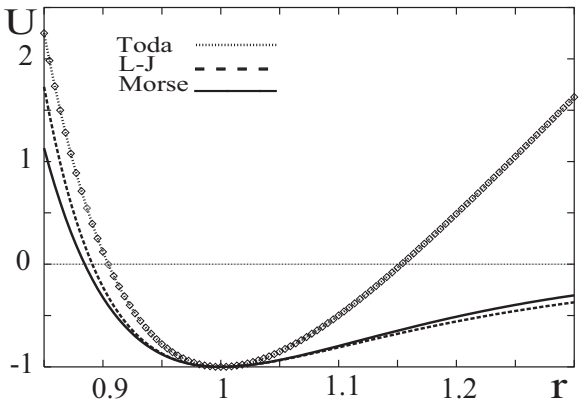

FIG. 1. LJ, Morse, and Toda potentials rescaled around their minima in such a way that the first three derivatives around the minimum are the same for all potentials to allow easy comparison of their repulsive parts.

is that of Alder *et al.* [18]. Their interest focused on a two-dimensional (2D) Hamiltonian with both on-site Coulomb repulsion and hopping probabilities that depend on dynamically varying separations of neighboring lattice sites. They obtained an equilibrium phase diagram as a function of density, electron-electron, and electron-phonon interaction strength. Alder *et al.* [18] did not consider anharmonicity along the lattice and did not incorporate breathers in the dynamics, but otherwise their model Hamiltonian was similar to that used by Cruzeiro-Hansson *et al.* [13], albeit in 2D. Other interesting works worth mentioning in view of what follows are the studies of mobile polarons in a Holstein-Hubbard model by Proville and Aubry [19] and Bonca *et al.* [20], and the work on bipolaron phase diagrams for the same model by Dorignac *et al.* [21].

In common with the model studied by Cruzeiro-Hansson *et al.* [13], here the intrinsic anharmonicity of lattice vibrations, albeit using a Morse potential, is considered (Fig. 1) (or more precisely, an adapted Morse-Toda potential [22]). This permits considering solitons moving along the nonlinear lattice. At variance with Cruzeiro-Hansson *et al.* [13], on-site nonlinear dynamics is not explicitly incorporated.

The outline of the paper is as follows. In the next section, we introduce the Davydov-Hubbard model system used herein. Localized two-electron soliton solutions are derived with the help of a variational approach minimizing the energy of the electron lattice system. Section III is devoted to a study of the time evolution of the electron soliton compounds focusing on coherent transport of paired electrons. Finally, we summarize and discuss our results.

II. THE DAVYDOV-HUBBARD SYSTEM

We investigate a one-dimensional periodic lattice chain of molecules coupled by Morse forces in which two (interacting) excess electrons have been injected. Our model Hamiltonian of charge transport in the system consists of the following two parts:

$$H = H_{\mathrm{el}} + H_{\mathrm{lattice}}. \tag{1}$$

H_{el} describes quantum mechanically the electron transport over the molecules in the context of a tight-binding system, and H_{lattice} represents the classical dynamics of longitudinal vibrations of the molecules, viz. the deformations of the corresponding bonds between them. The electronic system is given by the 1D Hubbard Hamiltonian,

$$H_{\mathrm{el}} = -\sum_{n,\sigma} (V_{nn-1}\hat{a}^{+}_{n\sigma}\hat{a}_{n-1\sigma} + V_{nn+1}\hat{a}^{+}_{n\sigma}\hat{a}_{n+1\sigma}) + U\sum_{n} \hat{a}^{+}_{n\uparrow}\hat{a}_{n\uparrow}\hat{a}^{+}_{n\downarrow}\hat{a}_{n\downarrow}. \tag{2}$$

The index $n \in [1,N]$ denotes the site of the nth molecule on the lattice, and σ determines the spin of an electron, which can be up or down. The standard Fermion operator $\hat{a}^{+}_{n\sigma}$ creates an electron with spin σ at site n, and $\hat{a}_{n\sigma}$ annihilates the electron. The symbol V_{nn-1} denotes the transfer-matrix element (its value is determined by an overlap integral) being responsible for the nearest-neighbor transport of the electron along the chain. The second term in Eq. (2) represents the on-site electron-electron interaction due to Coulomb repulsion related with the positive parameter U.

The lattice part of the Hamiltonian, H_{lattice}, models dynamical longitudinal changes of the equilibrium positions of the molecules yielding alterations of the length of bonds. The dynamics can appropriately be modeled by Morse potentials. The Hamiltonian of the H_{lattice} is given by

$$H_{\mathrm{lattice}} = \sum_{n} \left\{ \frac{p_n^2}{2M} + D\{1 - \exp[-B(q_n - q_{n-1})]\}^2 \right\}. \tag{3}$$

The coordinates q_n quantify the displacements of the molecules from their equilibrium positions along the molecular axis. D is the breakup energy of a bond, B is the range parameter of the Morse potential (the stiffness), and M denotes the mass of a molecular unit. The Morse potential exhibits an exponential-repulsive part preventing the crossover of neighboring lattice particles (molecules) for large displacements. Note that, with an expansion of the exponential functions, one recovers in lowest order the harmonic limit used in the Davydov model [7–10]. Besides, as shown in Fig. 1, there is not much difference between the Morse exponential and the $1/r^{12}$ LJ repulsion. As mentioned earlier, Cruzeiro-Hansson *et al.* [13] have considered the coupling of a Hubbard Hamiltonian (describing two correlated electrons of opposite spin) to dispersive phonons in a classical nonlinear lattice, the latter being of $1/r^{12}$ Lennard-Jones type. Emphasis is put on pair formation when a second additional electron is injected into the state of a single (standing) electron coupled to the lattice. Interesting effects occur such as an enhancement of localization when a nonlinear lattice mode (a breather) couples to the two-electron state in comparison with a much weaker electron localization in a harmonic lattice. Furthermore, the beneficial role of nonlinearity involved in the lattice for charge transport has been demonstrated in [23,24]. The lattice dynamics, where the units are coupled via Morse potentials, possesses properties similar to that of the Toda chain by suitably rescaling parameters [22]. In particular, to quite a good approximation, stable solitonic lattice deformations exist that are utilized as carriers for even supersonic charge transport as described in [23,24]. In the current paper, this idea is extended to the case of two correlated electrons being embedded in the nonlinear lattice of Morse-Toda type.

The interaction between the electronic and the vibrational degrees of freedom yields modifications of the electronic parameters V_{nn-1} due to the displacements of the molecules from their equilibrium positions. To be precise, the transfer-matrix elements V_{nn-1} are supposed to depend on the relative distance between two consecutive molecules on the chain in the following exponential fashion:

$$V_{nn-1} = V_0 \exp[-\alpha(q_n - q_{n-1})]. \tag{4}$$

The quantity α regulates how strong V_{nn-1} is influenced by the relative displacement of lattice units, $r_n = q_n - q_{n-1}$, or in other words, it determines the coupling strength between the electron and the lattice system. On the other hand, the actual charge occupation has its (local) impact on the longitudinal

distortion of the molecular chain. Note that here the exponential form of the electron-lattice interaction accounts for both small and large displacements of the lattice units, thus going beyond the range of harmonic interaction considered in earlier studies.

We pass to a dimensionless representation by introducing suitable scales. Time is scaled as $\tilde{t}=\Omega_{\text{Morse}}t$, with $\Omega_{\text{Morse}}=\sqrt{2DB^2/M}$ being the frequency of harmonic oscillations around the minimum of the Morse potential. The energy of the system is measured in units of the depth of the Morse potential, i.e., $H\to H/(2D)$. The dimensionless representation of the remaining variables and parameters of the system follows from the relations

$$\tilde{q}_n = Bq_n, \quad \tilde{p}_n = \frac{p_n}{\sqrt{2MD}}, \quad \tilde{V} = \frac{V_0}{2D}, \tag{5}$$

$$\tilde{\alpha} = \frac{\alpha}{B}. \tag{6}$$

In what follows, the tildes are omitted.

The exact two-electron wave function for the electron-lattice Hamiltonian (2) and (3) is given by the singlet state

$$|\psi(t)\rangle = \sum_{m,n} \phi_{mn}(\{p_m\},\{q_m\})\hat{a}^+_{m\uparrow}\hat{a}^+_{n\downarrow}|0\rangle, \tag{7}$$

where $|0\rangle$ is the vacuum state (containing no electrons) and ϕ_{mn} denotes the probability amplitude for an electron with spin up to occupy site m while an electron with spin down is at site n. The symmetric $\phi_{mn}=\phi_{nm}$ probability amplitudes are normalized $\Sigma_{mn}|\phi_{mn}|^2=1$ and depend further on the set of lattice variables $(\{p_m\},\{q_m\})$.

To obtain the equations of motion for the probability amplitudes, the wave function (7) is inserted into the Schrödinger equation for the Hamiltonian (2) and (3), and the evolution of the lattice variables is derived from the Hamiltonian principle related with the classical energy functional $\mathcal{E}^2=\langle\psi|H|\psi\rangle$ yielding the following set:

$$\begin{aligned} i\frac{d\phi_{mn}}{dt} = &-\tau\{\exp[-\alpha(q_{m+1}-q_m)]\phi_{m+1n} \\ &+ \exp[-\alpha(q_m-q_{m-1})]\phi_{m-1n} \\ &+ \exp[-\alpha(q_{n+1}-q_n)]\phi_{mn+1} \\ &+ \exp[-\alpha(q_n-q_{n-1})]\phi_{mn-1}\} + \bar{U}\phi_{mn}\delta_{mn}, \end{aligned} \tag{8}$$

$$\begin{aligned} \frac{d^2q_n}{dt^2} = &[1-\exp\{-(q_{n+1}-q_n)\}]\exp[-(q_{n+1}-q_n)] \\ &-[1-\exp\{-(q_n-q_{n-1})\}]\exp[-(q_n-q_{n-1})] \\ &+\alpha V\exp[-\alpha(q_{n+1}-q_n)]\sum_m\{[\phi^*_{mn+1}\phi_{mn}+\phi^*_{mn}\phi_{mn+1}] \\ &+[\phi^*_{n+1m}\phi_{nm}+\phi^*_{nm}\phi_{n+1m}]\} \\ &-\alpha V\exp[-\alpha(q_n-q_{n-1})]\sum_m\{[\phi^*_{mn}\phi_{mn-1}+\phi^*_{mn-1}\phi_{mn}] \\ &+[\phi^*_{nm}\phi_{n-1m}+\phi^*_{n-1m}\phi_{nm}]\}. \end{aligned} \tag{9}$$

The adiabaticity parameter $\tau=V/(\hbar\Omega_{\text{Morse}})$, appearing on the right-hand side (r.h.s) of Eq. (8), determines the degree of time-scale separation between the (fast) electronic and (slow) acoustic phonon or soliton processes. We further introduce the notation $\bar{U}=U/\hbar\Omega_{\text{Morse}}$ and drop the overbar in what follows. For illustration (unless stated otherwise), the following values are used: $\tau=10$, $V=0.1$, and $\alpha=1.75$ [24].

To establish a nonlinear charge-transport mechanism, one proceeds as in the single quantum particle case [23,24] and constructs as a first step localized stationary solutions of the coupled system (8) and (9), where one uses an adiabatic approach. To this end one notes that due to the fact that the lattice motion is slow compared to the electron motion (large adiabaticity parameter τ), the inertia in Eq. (9) is negligible so that the adiabatic approximation applies. Solutions of the stationary Schrödinger equation, associated with standing electrons, are obtained from Eq. (8) with the substitution $\phi_{mn}(t)=\Phi_{mn}\exp(-i\omega t)$ with real-valued amplitudes Φ_{mn} and where ω is the corresponding spectral parameter. The energy of the system is then given by

$$\begin{aligned} E = &\sum_n \frac{1}{2}\{1-\exp[-(q_n-q_{n-1})]\}^2 \\ &-2V\sum_{m,n}\{\exp[-\alpha(q_m-q_{m-1})]\Phi_{mn}\Phi_{m-1n} \\ &+\exp[-\alpha(q_n-q_{n-1})]\Phi_{mn}\Phi_{mn-1}\}+U\sum_{m,n}\Phi^2_{mn}\delta_{mn}, \end{aligned} \tag{10}$$

and the stationary equations are derived according to

$$\frac{\partial E}{\partial q_n}=0, \quad \frac{\partial}{\partial\Phi_{mn}}\left(E+\omega\sum_{m,n}\Phi^2_{mn}\right)=0. \tag{11}$$

For the localized electronic solution, one uses a simple trial function (see also [21]),

$$\phi^{(l)}_{mn} = A_l[\eta^{|m|+|n-l|}+\eta^{|m-l|+|n|}], \tag{12}$$

where the variational parameter $0<\eta<1$ gives the width of the solution, which is supposed to be localized with an inter-electron distance l. The coefficient A_l follows from the normalization condition and is evaluated as

$$A_l = \frac{1}{\sqrt{2(s_0^2+s_l^2)}}, \tag{13}$$

with

$$s_l = \frac{\eta^{|l|}}{1-\eta^2}[(|l|+1)-(|l|-1)\eta^2]. \tag{14}$$

The localized two-electron solution is connected with lattice deformations that are supposed to be of the form of two superimposed Toda solitons,

$$\exp[-(q_n - q_{n-1})] = +[1 + \sinh^2 \kappa \cosh^{-2}(\kappa n)] + \{1 + \sinh^2 \kappa \cosh^{-2}[\kappa(n-l)]\}, \tag{15}$$

where κ is treated as a variational parameter. Note that likewise for the electron pair, one assumes also that the distance between the soliton centers is l. The total variational energy is then expressed as

$$\begin{aligned}\Gamma = & \frac{1}{2}\sum_n \left(\frac{\sinh^4 \kappa}{\cosh^4(\kappa n)} + \frac{\sinh^4 \kappa}{\cosh^4[\kappa(n-l)]} \right) \\ & - 2VA_l^2 \sum_{m,n} \left\{ \left(2 + \frac{\sinh^2 \kappa}{\cosh^2(\kappa m)} + \frac{\sinh^2 \kappa}{\cosh^2[\kappa(m-l)]} \right)^{\alpha} \right. \\ & \times [\eta^{|m|+|n-l|} + \eta^{|m-l|+|n|}][\eta^{|m-1|+|n-l|} + \eta^{|m-1-l|+|n|}] \\ & + \left(1 + \frac{\sinh^2 \kappa}{\cosh^2(\kappa n)} + \frac{\sinh^2 \kappa}{\cosh^2[\kappa(n-l)]} \right)^{\alpha} \\ & \left. \times [\eta^{|m|+|n-l|} + \eta^{|m-l|+|n|}][\eta^{|m|+|n-1-l|} + \eta^{|m-l|+|n-1|}] \right\} \\ & + UA_l^2 \sum_{m,n} [\eta^{|m|+|n-l|} + \eta^{|m-l|+|n|}]^2 \delta_{mn}. \end{aligned} \tag{16}$$

For a given set of system parameters α and V, the global minimum of Γ, giving the lowest energy configuration, is searched for in the three-parameter space (κ, l, η). The probability for one electron to be in site n with spin up and spin down, respectively, is determined by

$$\rho_{n\uparrow} = \langle \psi | \hat{a}_{n\uparrow}^{+} \hat{a}_{n\uparrow} | \psi \rangle = \sum_k |\phi_{nk}|^2, \tag{17}$$

$$\rho_{n\downarrow} = \langle \psi | \hat{a}_{n\downarrow}^{+} \hat{a}_{n\downarrow} | \psi \rangle = \sum_k |\phi_{kn}|^2. \tag{18}$$

Typical electron probability distributions [because of the symmetry it holds that $\rho_{n\uparrow} = \rho_{n\downarrow}$ and we plot half the electron density at a site n defined as $\rho_n = \frac{1}{2}\Sigma_k(|\phi_{kn}|^2 + |\phi_{nk}|^2)$ and the corresponding profile of displacements of the molecules] are depicted in Fig. 2 for three different values of the repulsive interaction strength U. The corresponding localized compound comprises an exponentially localized two-electron state, and the associated pair of kink-shape topological lattice deformations that are represented as $\exp[-(q_n - q_{n-1})]$ are of a bell shape. The latter are referred to herein as the lattice solitons. Increasing the repulsive (Coulomb) Hubbard interaction has the impact that the interelectron distance (and accordingly also the distance between the centers of the solitons) gets larger. At the same time the degree of localization reduces, i.e., broader profiles of lower peak values result. Notably, the localized solutions are of fairly broad width and thus are expected to be mobile when kinetic energy of an appropriate form is added. In more detail, for a low value $U = 0.05$ the electron probability density is single-peaked where the peak is shared by two neighboring sites to either side of which the localized pattern decays. Doubling the value to $U = 0.1$ causes a split up of ρ_n into a double-peaked structure of lesser amplitude than in the preceding case. The

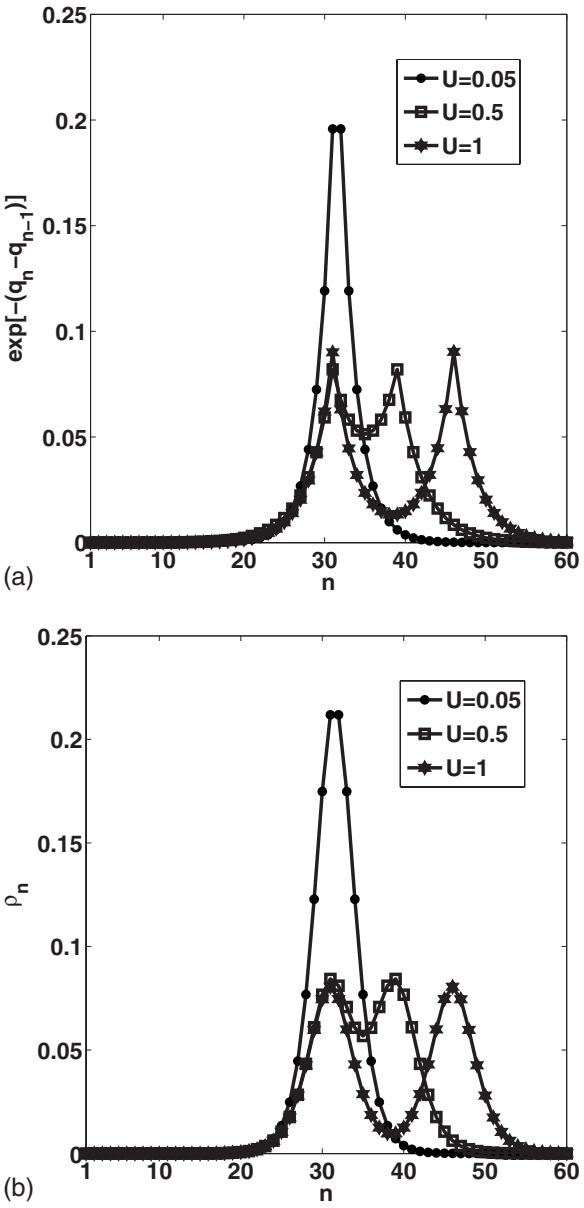

FIG. 2. Initial profile of the localized lattice deformation (top panel) and electron probability distribution (bottom panel) realizing a minimum of the variational energy for three different values of the Hubbard parameter U as indicated in the plots. The remaining parameter values are $\alpha = 1.75$ and $V = 0.1$.

interelectron distance amounts to $l = 8$. With a further increased value of U, the two peaks of ρ get further apart from each other while the degree of localization is further reduced (see also below in Fig. 4). Crucially for $U \gtrsim 0.9$, the interelectron distance l exceeds the width of either of the two peaks of the electron probability density. Therefore, the two electrons can no longer be regarded as paired. Those features of the electron probability are equivalently exhibited by the soliton patterns, that is, the larger the repulsive interaction strength U is, the less is the lattice compression reflected in the width and amplitude of the soliton patterns. For a more comprehensive representation, Fig. 3 shows the binding energy $E_{\text{binding}} = \Gamma - 2E_1$ (where Γ is the minimal energy attained in the correlated two-electron lattice system and $2E_1$ is

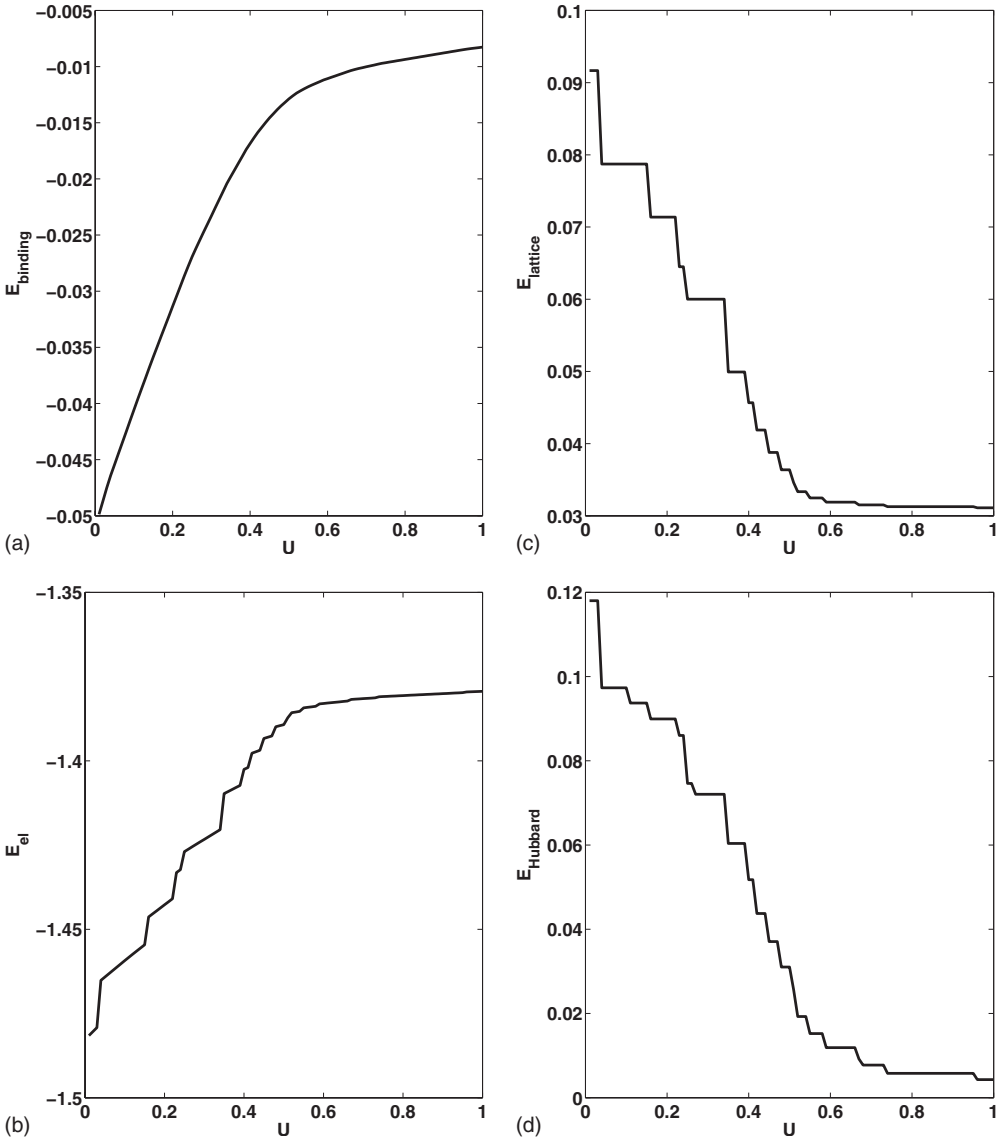

FIG. 3. Binding energy, electron energy, lattice energy, and correlation energy as a function of the repulsive Hubbard interaction strength U. The remaining parameter values are $\alpha=1.75$ and $V=0.1$.

the energy of two single localized electron soliton states being apart as much as possible from each other in the lattice) as a function of the (Coulomb) Hubbard interaction strength U. Furthermore, the partial electron energy and lattice energy as given by the expressions (2) and (3), respectively, as well as the electron correlation energy E_{Hubbard}, determined by only the last term in Eq. (2), are depicted, respectively. In compliance with the findings reported above with increasing Hubbard interaction strength (for which the degree of localization is lowered), the binding energy decreases. Likewise the electron energy E_{el} (starting from far below the lower edge of the energy band of extended states) gets eventually close to the value of the lower edge of the energy band of extended states. Correspondingly, the diminishing lattice energy E_{lattice} upon increasing U goes along with a reduction of the degree of lattice deformation as noted also above. The intensity of the electron correlation is manifested in the behavior of E_{Hubbard} as a function of U, and one notices a rapid decrease of E_{Hubbard} for growing U. In Fig. 4, the interelectron distance as a function of the repulsive (Coulomb) Hubbard-interaction strength U is shown. From the perspective of the energy distribution, we mention that at the transition from correlated to uncorrelated electron states, the energy saving coming from the interaction of the paired electron state with the lattice no longer exceeds the energy contained in the repulsion term and the contribution of the repulsive energy becomes so dominant that the paired state is no longer energetically favorable. Remarkably, in Figs. 3 and 4 there occur several intervals of U values for which the partial energies as well as the interelectron distance exhibit plateaus.

III. MOVING ELECTRON-PAIR SOLITON COMPOUNDS

Having obtained the lowest energy configuration with the help of the variational approach in the previous section, now the dynamical behavior of the localized electrons coupled with the corresponding lattice deformations is investigated.

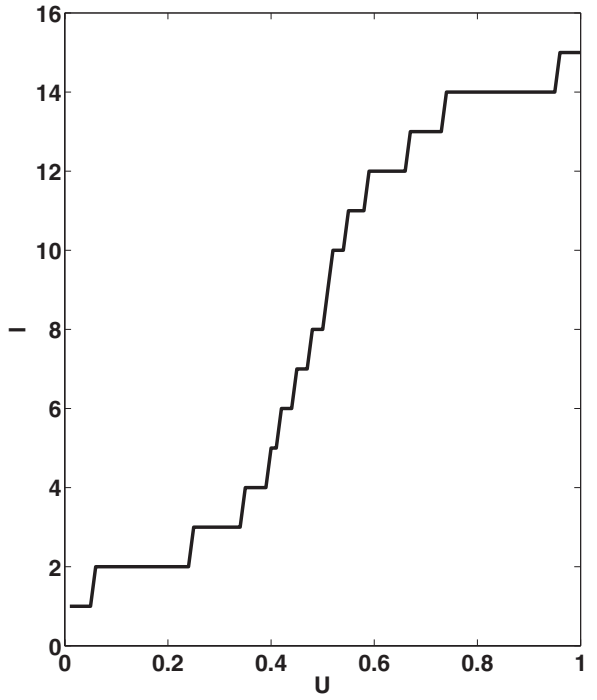

FIG. 4. Interelectron distance attained in the minimum energy configuration in dependence on the Hubbard parameter U. The remaining parameter values are $\alpha=1.75$ and $V=0.1$.

Motion of the lattice soliton is achieved with the excitation of the Toda soliton momenta according to

$$p_n = 2\sinh(\kappa)/\kappa(\exp[2\kappa(n-1)]/\{1+\exp[2\kappa(n-1)]\} - \exp[2\kappa(n-l)]/\{1+\exp[2\kappa(n-l)]\}) + 2\sinh(\kappa)/\kappa(\exp[2\kappa(n-l-1)]/\{1+\exp[2\kappa(n-l-1)]\} - \exp[2\kappa(n-l)]/\{1+\exp[2\kappa(n-l)]\}). \quad (19)$$

One should bear in mind that while in this way the lattice is equipped with kinetic energy, the electrons are presented as a standing state (see above). Moreover, in the case of vanishing electron lattice interaction strength, $\alpha=0$, the lattice solitons move form-invariant (apart from negligibly small radiation) with uniform velocity along the lattice resembling the behavior of the initially exact Toda solitons [25]. For the system of a single standing electron coupled to the Morse lattice ($\alpha\neq 0$), coherent charge transport is mediated by a soliton carrier as illustrated in [23,24]. The question now is whether such a soliton-assisted transport mechanism is achievable in the more complex situation of two correlated standing electrons in the lattice. We integrated the system (8) and (9) with $N=61$ lattice sites using a fourth-order Runge-Kutta scheme where periodic boundary conditions are imposed. We checked the accuracy of our computations by monitoring the conservation of the norm $\Sigma_{mn}|\phi_{mn}(t)|^2=1$ as well as the conservation of the total energy. The spatio-temporal evolution for a relatively low repulsive interaction strength, $U=0.05$, is illustrated in Fig. 5. The lattice deformation solitons travel with uniform but *subsonic* velocity along the lattice retaining their localized profile despite the emission of small-amplitude waves to either side in the beginning. Likewise the localized shape of the electron pair probability distribution as well as the interelectron distance of $l=1$ are maintained throughout the simulation time. Apparently part of the energy contained initially in the lattice deformation is distributed in the electronic degree of freedom with the result that the height of the electron probability density increases. On the other hand, the reduction of the lattice deformation energy lowers the velocity of the corresponding solitons. For an increased repulsive interaction strength, $U=0.1$, the localized electron pair probability distribution and the lattice soliton pair consist of two peaks being a distance of $l=8$ sites apart from each other. Interestingly, as seen in Fig. 6, in an early stage of the time evolution the two peaks of the electron probability distribution and the lattice pair approach each other leading to a drastic increase of localization in a single peak state in the electron and lattice component, which then travel in unison with apparent

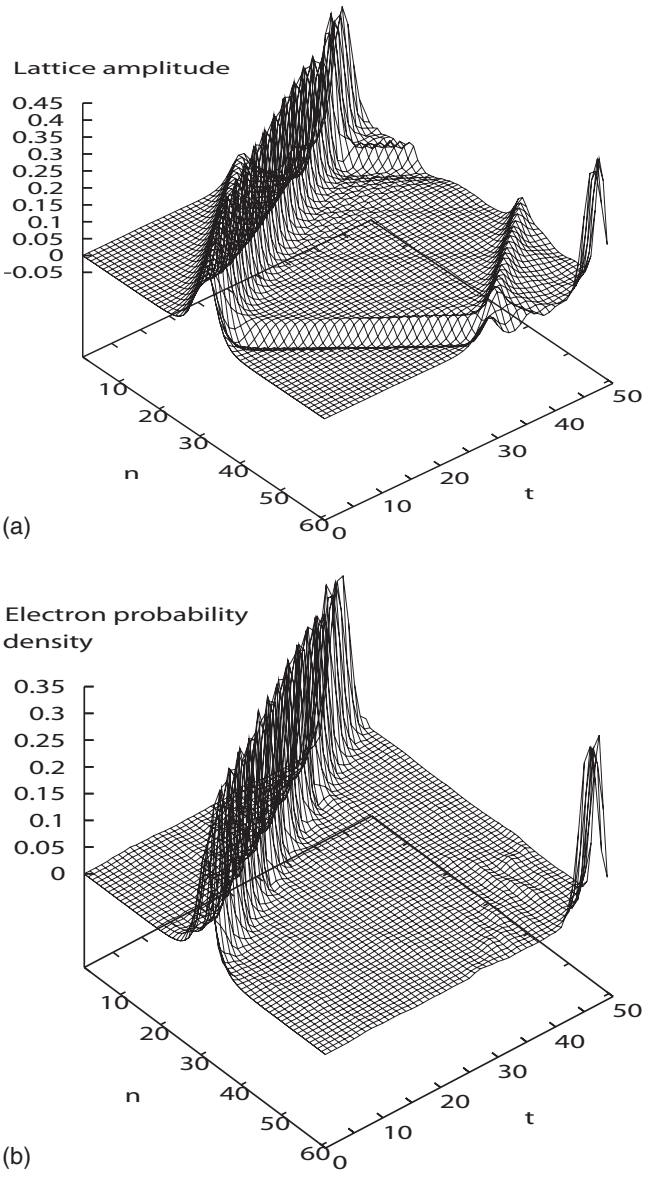

FIG. 5. Spatio-temporal evolution of a lattice soliton pair (top panel) and the electron probability distribution (bottom panel). The parameter values are $\alpha=1.75$, $V=0.1$, and $U=0.05$.

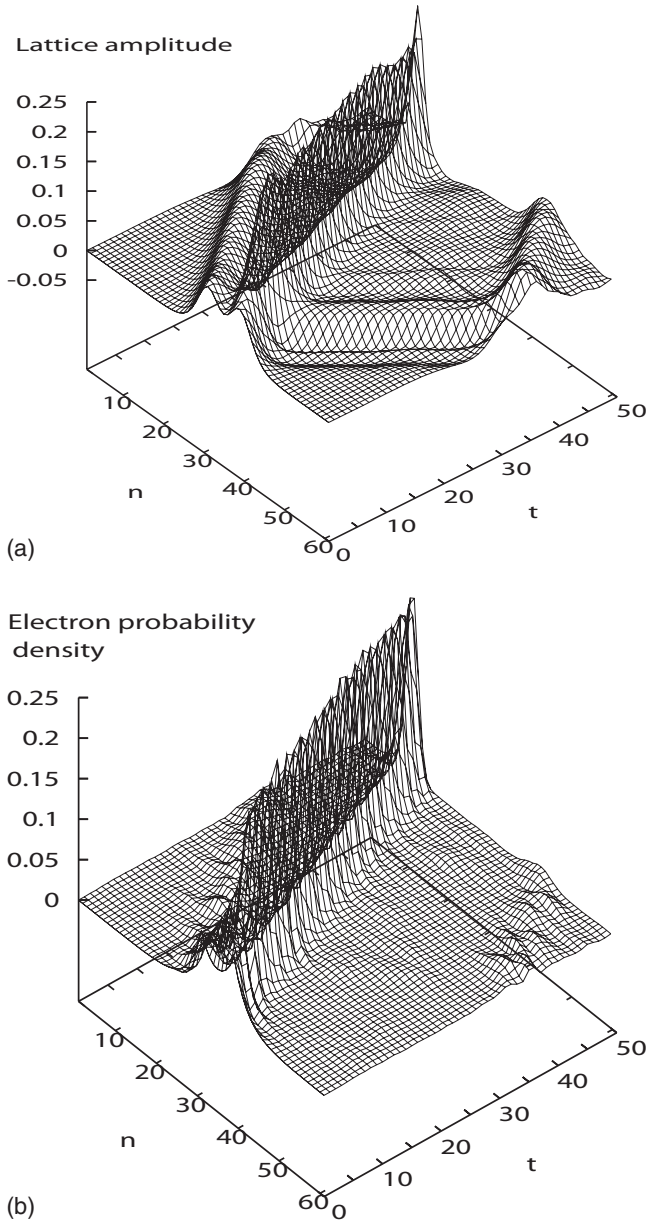

FIG. 6. Spatio-temporal evolution of a lattice soliton (top panel) and the electron probability distributions (bottom panel). The parameter values are $\alpha=1.75$, $V=0.1$, and $U=0.1$.

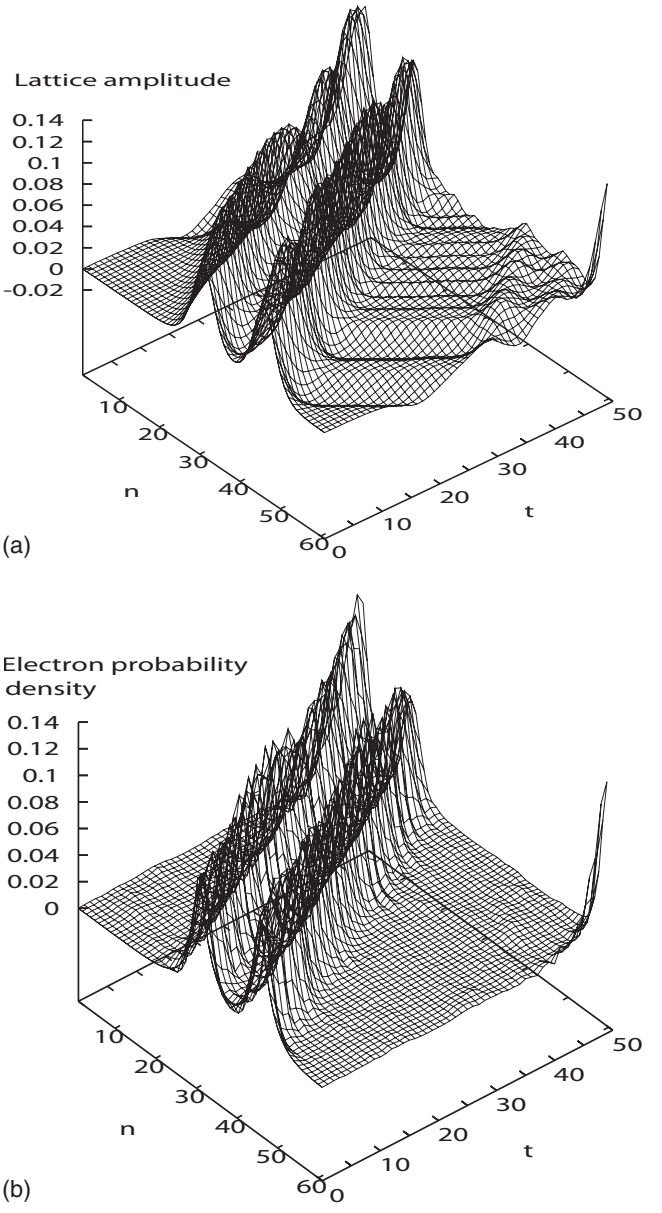

FIG. 7. Spatio-temporal evolution of a lattice soliton (top panel) and the electron probability distributions (bottom panel). The parameter values are $\alpha=1.75$, $V=0.1$, and $U=1$.

stability along the lattice. Thus, starting from a pronounced double-peak configuration, the dynamics causes the two peaks to merge, and subsequently coherent transport of a strongly single-peaked electron probability distribution (strongly coupled electron pair) achieved by a traveling lattice soliton carrier occurs.

However, for large repulsive interaction strength $U=1$, for which the interpeak distance amounts to a value $l=15$, virtually no dynamical changes of the initial localized profiles, apart from the emission of small portions of linear waves from them, is observed (see Fig. 7). Thus, in this case the Coulomb repulsion is too strong so that profile narrowing of the localized electron probability distribution cannot take place.

Finally, we studied also higher interaction strengths between the electrons and the lattice deformations. Interestingly, it turned out that there result *supersonic* moving paired electron lattice soliton compounds as illustrated in Fig. 8 for interaction strength $\alpha=2$ and transfer matrix element $V=0.25$ for which an interelectron distance $l=1$ is attained. The plot clearly exhibits a large-amplitude excitation in the electron probability density (although its amplitude diminishes weakly in the course of time) as well as the lattice amplitudes moving in unison with *supersonic* velocity leaving behind the phonon waves that have been initially emitted from them. Clearly, due to decoherence and dissipation, the lifetime of a bound electron-soliton state is limited. Nevertheless, from the simulations performed in Ref. [23] one infers that the lifetime of bound states between solitons and electrons can last up to a hundred picoseconds during which

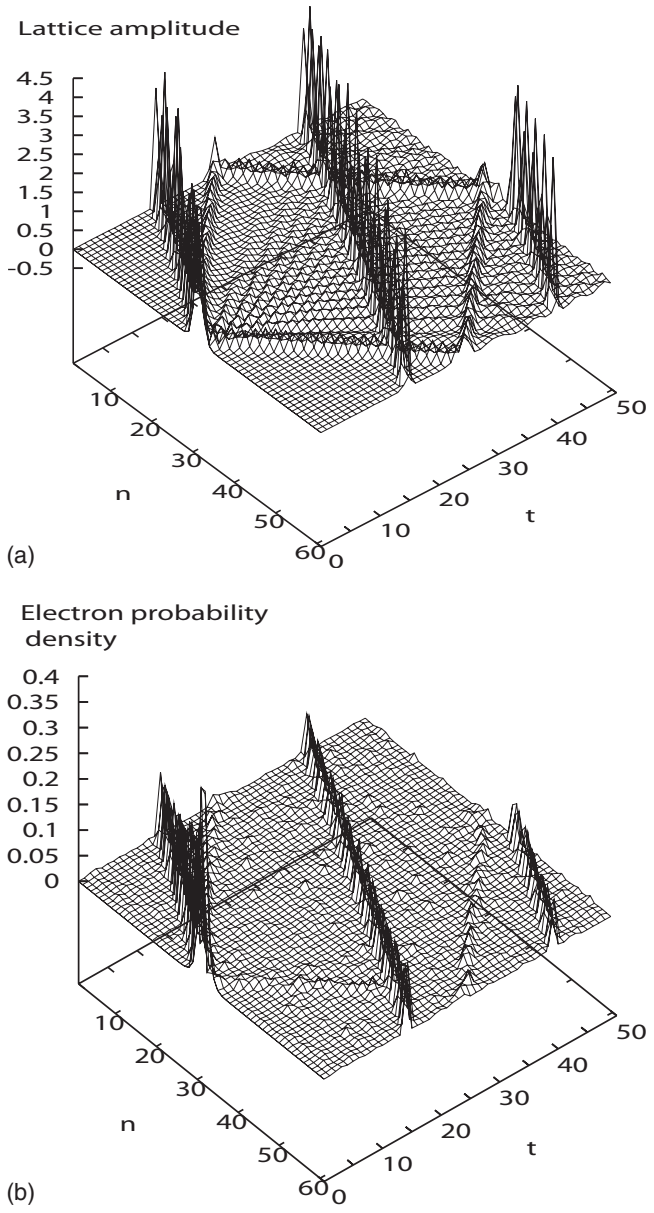

FIG. 8. Spatio-temporal evolution of the lattice solitons (top panel) and the electron probability distributions (bottom panel) traveling with supersonic velocity. The parameter values are $\alpha=2$, $V=0.25$, and $U=0.1$.

a distance of ~ 40 Å is traversed on the molecular chain. This holds true also for the paired states as confirmed by the simulations presented in the current paper.

IV. CONCLUSIONS

We studied the time evolution of two correlated electrons of opposite spin moving in a one-dimensional lattice chain within a mixed quantum-classical approach. While the electron dynamics is treated quantum mechanically using the Hubbard Hamiltonian, the units of the classical lattice are coupled via Morse-Toda potentials. Interaction between the electrons and the lattice stems from the modulation of the electronic transfer-matrix element by the relative displacements between two lattice sites. The correlation between the electrons is due to the repulsive Coulomb interaction and is accounted for in the on-site Hubbard term (for an alternative approach, see [26]). Concerning the more realistic case of a solid-state system involving the Fermi sea, the following remark is in order: In the current paper, only two electrons in a one-dimensional lattice are considered and a solid-state system with a sea of electrons is beyond the scope of the present study. However, one may say that if the electrons are degenerate, then it is expectable that bound states persist to a certain extent, since the degeneration weakens the Coulomb repulsion.

Attention was paid to a coherent charge-transport mechanism where a pair of lattice solitons is supposed to serve as the carrier of the two correlated electrons forming a pair that is represented by a localized probability distribution. Such localized electron soliton compounds were searched for by minimizing an associated functional for the potential energy. It was illustrated that in dependence of the strength of the repulsive (Coulomb) Hubbard interaction strength, the electron probability distribution can be either single-peaked or double-peaked. In the former case, the single peak of the electron probability distribution is shared symmetrically by two neighboring sites, while in the latter case the two peaks get farther away from each other as the repulsive (Coulomb) Hubbard interaction strength increases. Accordingly, the distance between the centers of the two charge-carrying lattice solitons adapts to the interelectron distance. Equipping the soliton pair with kinetic energy, the motion of the localized electron soliton compound is initiated. In dependence of the parameters of the model system, two regimes of coherent transport were found. For relatively small value of the transfer-matrix element and moderate coupling strength between the electrons and the lattice, the charge transport proceeds with subsonic velocity. Remarkably, increasing the values of the two aforementioned parameters beyond a respective critical value causes the supersonic transport of paired electrons. Our results generalize an earlier finding by Zolotaryuk *et al.* [17], who identified a supersonic transport mode where two soliton peaks can attach to a polaron with a single electron creating together with it a coupled or dynamic bound state.

Finally, in comparison with the study by Cruzeiro-Hansson *et al.* [13], one notes that in their treatment of the lattice evolution, intrinsic nonlinearity occurs in a twofold way: There is the anharmonic treatment of coupling interaction between the lattice units using the $1/r^{12}$ LJ potential, and furthermore, quartic on-site potentials are incorporated. We underline that in our study, the on-site nonlinearity, which is the source for breather formation in [13], is absent. However, the model in [13] and ours have the nonlinear coupling interaction between the lattice sites in common. As already noted above, the corresponding anharmonic LJ and Morse potentials share a virtually equal repulsive part and hence support solitonlike solutions. In addition, the electron lattice interaction is responsible for another nonlinear effect, namely trapping of the electron(s) through the resulting polaron formation. (We recall that this happens also in the case of linear coupling interaction between the lattice sites, i.e., when soliton solutions of the lattice itself are impossible.)

Distinct to our present study, Cruzeiro-Hansson *et al.* [13] focused their interest on the *formation process* of a pair of correlated quasiparticles arising when an additional quasiparticle is injected into the system state of a single quasiparticle coupled to the nonlinear lattice. The most stable state is then supposed to be attained for zero kinetic energy. Discussing the stability of the static minimum energy configurations under the impact of the additional on-site lattice nonlinearity term, they noticed that the presence of the latter supports the formation of strong lattice deformation in the form of a standing breather around the site where the two quasiparticles reside. This turns out to enhance the stability of the paired quasiparticle state. In contrast, this paper is concentrated on the *soliton-assisted transport mechanism* of correlated electrons. Departing from Cruzeiro-Hansson *et al.* [13], lattice solitons (hence with an amount of initial kinetic energy) together with the associated (standing) localized paired electron as initial conditions were used. It is demonstrated that for vanishing on-site nonlinearity (viz., zero elasticity of the on-site potential), but with the presence of nonlinear coupling interaction between the lattice units, the coupled electron lattice dynamics provides a stable transport mechanism of paired electrons. Currently we are investigating the issue of mobility of the localized electron pair lattice soliton compound in the system with on-site lattice potentials.

ACKNOWLEDGMENTS

This research was sponsored in part by the European Union under Grant No. SPARK-II-FP7-ICT-216227 and by the Spanish Government under Grant No. MEC-VEVES-FIS2006-01305.

[1] L. D. Landau, Phys. Z. Sowjetunion **3**, 664 (1933).
[2] S. I. Pekar, Zh. Eksp. Teor. Fiz. **16**, 335 (1946); L. D. Landau and S. I. Pekar, *ibid.* **18**, 419 (1948).
[3] H. Fröhlich, Adv. Phys. **3**, 325 (1954) (and references therein).
[4] T. Holstein, Ann. Phys. (N.Y.) **8**, 325 (1959).
[5] See, e.g., *Polarons in Ionic Crystals and Polar Semiconductors*, edited by J. T. L. Devreese (North-Holland, Amsterdam, 1972).
[6] R. P. Feynman, Phys. Rev. **97**, 660 (1955).
[7] A. S. Davydov, J. Theor. Biol. **38**, 559 (1973); A. S. Davydov and N. I. Kislukha, Sov. Phys. JETP **44**, 571 (1973); A. S. Davydov, Sov. Phys. Usp. **25**, 898 (1982).
[8] A. S. Davydov, *Solitons in Molecular Systems*, 2nd ed. (Reidel, Dordrecht, 1991).
[9] *Davydov's Solitons Revisited*, edited by P. L. Christiansen and A. C. Scott (Plenum, New York, 1991).
[10] A. C. Scott, Phys. Rep. **217**, 1 (1992).
[11] M. G. Velarde, W. Ebeling, and A. P. Chetverikov, Int. J. Bifurcation Chaos (to be published).
[12] M. G. Velarde, Int. J. Comput. Appl. Math. (to be published).
[13] L. Cruzeiro-Hansson, J. C. Eilbeck, J. L. Marin, and F. M. Russell, Eur. Phys. J. B **42**, 95 (2004).
[14] *The Hubbard Model, A Reprint Volume*, edited by A. Montorsi (World Scientific, New York, 1992).
[15] T. P. Valkering, J. Phys. A **11**, 1885 (1978).
[16] G. Friesecke and J. A. D. Wattis, Commun. Math. Phys. **161**, 391 (1994).
[17] A. V. Zolotaryuk, K. H. Spatschek, and A. V. Savin, Phys. Rev. B **54**, 266 (1996).
[18] B. J. Alder, K. J. Runge, and R. T. Scalettar, Phys. Rev. Lett. **79**, 3022 (1997).
[19] L. Proville and S. Aubry, Physica D **113**, 307 (1998); Eur. Phys. J. B **11**, 41 (1999).
[20] J. Bonca, T. Katrasnik, and S. A. Trugman, Phys. Rev. Lett. **84**, 3153 (2000).
[21] J. Dorignac, J. Zhou, and D. K. Campbell, Physica D **216**, 207 (2006).
[22] A. P. Chetverikov, W. Ebeling, and M. G. Velarde, Eur. Phys. J. B **51**, 87 (2006).
[23] D. Hennig, C. Neißner, M. G. Velarde, and W. Ebeling, Phys. Rev. B **73**, 024306 (2006).
[24] D. Hennig, A. Chetverikov, M. G. Velarde, and W. Ebeling, Phys. Rev. E **76**, 046602 (2007).
[25] M. Toda, *Theory of Nonlinear Lattices*, 2nd ed. (Springer-Verlag, Berlin, 1989).
[26] M. G. Velarde and C. Neissner, Int. J. Bifurcation Chaos Appl. Sci. Eng. **18**, 885 (2008).